Interplay of Oxygen, Vitamin E, and Carotenoids in Radical Reactions following Oxidation of Trp and Tyr Residues in Native HDL_3 Apolipoproteins. Comparison with LDL. A Time-Resolved Spectroscopic Analysis†

Agnès Boullier,[‡,§,||] Jean-Claude Mazière,[§,‡,||] Paulo Filipe,[⊥] Larry K. Patterson,[#,‡] David M. Bartels,[#] Gordon L. Hug,[#] João P. Freitas,[⊥] René Santus,[▽,○] and Patrice Morlière*[,||,§,‡]

INSERM, ERI12, F-80054 Amiens, France, Université de Picardie Jules Verne, Faculté de Médecine et de Pharmacie, EA 2087, F-80036 Amiens, France, CHU Amiens Nord, Laboratoire de Biochimie, F-80054 Amiens, France, Faculdade de Medicina de Lisboa, Hospital Santa Maria, Clinica Universitária de Dermatologia, 1600 Lisbon, Portugal, University of Notre Dame, Radiation Laboratory, Notre Dame, Indiana 45556, INSERM, U697, F-75475 Paris, France, and Muséum National d'Histoire Naturelle, Département RDDM, F-75231 Paris, France

Received December 8, 2006; Revised Manuscript Received February 5, 2007

ABSTRACT: It has been recently shown that the inhibition of apolipoprotein A-I (apoAI) reverse cholesterol transport activity during oxidation of HDL by myeloperoxidase may involve myeloperoxidase electron transfer pathways other than those leading to tyrosine chlorination. To better understand how such mechanisms might be initiated, the role of semioxidized Tyr and Trp residues in loss of apoAI and apolipoprotein A-II (apoAII) integrity has been assessed using selective Trp and Tyr one-electron oxidation by $^{\bullet}Br_2^-$ radical-anions in HDL_3 as well as in unbound apoAI and apoAII. Behavior of these radicals in apolipoprotein B of LDL has also been assessed. Formation of semioxidized Tyr in HDL_3 is followed by partial repair during several milliseconds via reaction with endogenous α-tocopherol to form the α-tocopheroxyl radical. Subsequently, 2% of α-tocopheroxyl radical is repaired by HDL_3 carotenoids. With LDL, a faster repair of semioxidized Tyr by α-tocopherol is observed, but carotenoid repair of α-tocopheroxyl radical is not. Only a small fraction of HDL_3 particles contains α-tocopherol and carotenoids, which explains limited repair of semioxidized Tyr by α-tocopherol. All LDL particles normally contain multiple α-tocopherol and carotenoid molecules, and the lack of repair of α-tocopheroxyl radical by carotenoids probably results from hindered mobility of carotenoids in the lipid core. Western blots of γ-irradiated HDL_3 comparable to those reported for apoAI myeloperoxidase oxidation show that the incomplete repair of semioxidized Tyr and Trp induces apoAI and apoAII permanent damage including formation of a heterodimer of one apoAI with a monomeric apoAII at about 36 kDa.

HDL exhibits antiatherosclerotic effects through its participation in reverse cholesterol transport by taking up free cholesterol from peripheral tissues for delivery to liver and steroidogenic organs (*1*) and by inhibiting LDL oxidation (*2*). It is believed that HDL_3 and LDL oxidation *in vivo* occurs within lesions of the arterial wall, leading to formation of macrophage foam cells and, consequently, expression of atherosclerosis (*3*). Among the consequences of such oxidation, oxidized HDL_3 loses its ability to promote cholesterol efflux from such foam cells. There are several physiological pathways by which oxygen radicals may be generated to initiate these degenerative processes. For example, the NADH oxidase of phagocytes produces $^{\bullet}O_2^-$ radical-anions and H_2O_2. These reactive oxygen species can subsequently react, via Fenton-like reactions, with redox metal ions present in the locally inflamed area to produce the strongly oxidizing $^{\bullet}OH$ radical. Such species are also produced by peroxidases of phagocytes such as myeloperoxidase (MPO)[1] (*4*).

It has recently been shown that MPO binds selectively to apolipoprotein A-I (apoAI)[1], the major protein of HDL_3 in plasma (*5*). This interaction combined with the high chemical reactivity of the heme−H_2O_2 complex, which oxidizes inorganic (*e.g.* halides, $^{\bullet}NO$ and NO_2^-) as well as biological (*e.g.* oxidizable amino acids) substrates through competitive one- and two-electron transfer reactions (*6*), is believed to be responsible for the numerous amino acid derivatives of

† This work was supported by the Franco-Portuguese exchange programs GRICES-INSERM 2005−2006 and Pessoa 07958NF. Notre Dame Radiation Laboratory is supported by the Office of Basic Energy Sciences of the U.S. Department of Energy. This is document 4695 from the Notre Dame Radiation Laboratory.

* To whom correspondence should be addressed: INSERM ERI12, Laboratoire de Biochimie, CHU Amiens Nord, place Victor Pauchet, 80054 Amiens Cedex 1, France. Tel: + 33 3 22 66 86 69. Fax: + 33 3 22 66 89 17. E-mail: morliere.patrice@chu-amiens.fr.

‡ CHU Amiens Nord, Laboratoire de Biochimie.

§ Université de Picardie Jules Verne, Faculté de Médecine et de Pharmacie.

|| INSERM, ERI12.

⊥ Faculdade de Medicina de Lisboa, Clinica Universitária de Dermatologia.

University of Notre Dame, Radiation Laboratory.

▽ INSERM, U697.

○ Muséum National d'Histoire Naturelle, Département RDDM.

[1] Abbreviations: MPO, myeloperoxidase; apoAI, apolipoprotein A-I; TyrO•, semioxidized Tyr; •Trp, semioxidized Trp; apoAII, apolipoprotein A-II; apoB, apolipoprotein B; αTocOH, α-tocopherol; Car, carotenoids; αTocO•, α-tocopheroxyl radical.

10.1021/bi602530g CCC: $37.00
Published on Web 04/06/2007

apoAI observed upon oxidation by MPO. Among them, chlorination or nitration products of Tyr residues are found in human atherosclerotic lesions, and their systemic levels are considered as predictors of atherosclerotic risk (*5*).

Besides chlorination or nitration of Tyr residues, however, most recent studies point to the possibility that other important reactions may participate in oxidation of HDL_3. For example, the phenoxyl tyrosyl radical ($TyrO^{\bullet}$)[1] is produced either by one-electron oxidation of Tyr or by $^{\bullet}OH$ addition to its phenoxyl ring protein, and cross-linking through bityrosyl bridges formed by intermolecular recombination of $TyrO^{\bullet}$ has been described (*7*). Moreover, Peng et al. very recently suggested that formation of chlorolysine and/or mono- and dihydroxytryptophan from the four Trp residues of apoAI may be responsible for the MPO-induced loss of apoAI structure and activity (*8*). In this regard, the formation of Trp hydroxylation products may be expected to result from radical activity. Indeed, earlier radiation chemistry studies of $^{\bullet}OH$ radical reaction with aqueous Trp (*9*) demonstrated that both an adduct on the benzene ring and the neutral $^{\bullet}Trp$ radical (*10*) are produced by $^{\bullet}OH$ attack on the indole ring, with yields of 40 and 60%, respectively. Hence, in addition to chlorination and nitration of Tyr residues, it may be expected that formation of the $^{\bullet}Trp$ and $TyrO^{\bullet}$ radicals following $^{\bullet}OH$ radical formation by Fenton-like reactions or by the specific apoAI-MPO interaction (*5*) can contribute to the oxidative impairment of HDL_3. The goal of this study is to better understand how the lipoprotein environment may influence interplay of these radicals as well as dictate their reactions with other lipoprotein components. Within this context, the kinetic and spectral behavior of $^{\bullet}Trp$ and $TyrO^{\bullet}$, generated by $^{\bullet}Br_2^-$ oxidation (*11*) of Trp and Tyr residues in the apoAI and apolipoprotein A-II (apoAII)[1] of HDL_3, as well as in the apolipoprotein B (apoB)[1] of LDL, has been measured by pulse radiolysis on a time scale extending from tens of microseconds to tens of seconds. To aid in interpretation of lipoprotein behavior, parallel measurements have been carried out with isolated apoAI and apoAII. The roles played by other physiological components of the native particle, i.e., the antioxidants vitamin E (α-tocopherol, αTocOH)[1] and carotenoids (Car),[1] have also been examined. The sequence of reactions involved and the effect of oxygen on their kinetic parameters have been determined as well. It is observed that the hydrophobic αTocOH partially repairs apoAI and apoAII damage by reduction of $TyrO^{\bullet}$ radicals. Partial repair of α-tocopheroxyl ($\alpha TocO^{\bullet}$)[1] radicals by Car has been observed in HDL_3 but not in LDL. The long-term consequences of the imperfect repair of radical damage to apoAI, e.g., fragmentation and polymerization, have been examined by Western blots from HDL_3 samples treated by γ-irradiation under experimental conditions similar to those used in the time-resolved study.

EXPERIMENTAL PROCEDURES

Materials. All chemicals were analytical grade and were used as received from the suppliers. Delipidated and purified apoAI and apoAII were purchased from Biodesign International (Saco, ME). Goat anti-human apoAI and apoAII antibodies were purchased from Acris Antibodies (Hiddenhausen, Germany), and the rabbit anti-goat horseradish peroxidase conjugate was purchased from Santa Cruz Biotechnology (Santa Cruz, CA). The 10 mM, pH 7, phosphate buffer was prepared in pure water obtained with a reverse osmosis/deionization system from Serv-A-Pure Co. The water exhibits a resistivity of >18 MΩ cm^{-1} and a total organic content of <10 ppb.

Preparation of HDL_3 and LDL. Lipoproteins from pooled plasma of fasting healthy normolipidemic human volunteers were prepared in the presence of 0.5 mM EDTA by sequential ultracentrifugation at 105000*g*. HDL_3 was taken as the 1.125−1.210 density fraction whereas LDL was isolated in the 1.024−1.060 density fraction (*12*). The LDL and HDL fractions were free of apolipoprotein E. For all pulse radiolysis experiments, EDTA was removed by two cycles of dialyses against 2 l of 10 mM, pH 7, phosphate buffer described above but with addition of 0.1 M KBr at 4 °C beginning 24 h prior to the experiments. The absence of oxidation during the dialysis of LDL has been discussed in one of our earlier reports (*13*). There is no reason to believe that this behavior would be different in HDL. Unless otherwise stated, dialyzed lipoprotein solutions were diluted to 12.5 μM and 1.6 μM for HDL_3 and LDL, respectively, just before pulse radiolysis. HDL_3 concentration was estimated from its protein content on the basis of an average protein content of 2 apoAI and 1.5 apoAII per HDL_3 particle (*14*), i.e., ∼ 80 000 g of protein per mole of HDL_3. Absorbance spectra of lipoprotein solutions were recorded before and after pulse radiolysis experiments. Sets of measurements were made in July and again the following March. Freshly isolated lipoproteins, native HDL_3 and LDL, were obtained using blood samples from the same donors for each set, and similar data were obtained.

Western Blot. HDL_3 samples were analyzed by electrophoresis on a 12% SDS−polyacrylamide gel under reducing (*8*) and nonreducing conditions. The gels were either stained for protein with 0.25% Coomassie Blue or transferred onto a nitrocellulose membrane. The membrane was blocked with 5% fat free milk or bovine serum albumin in TBS (20 mM Tris HCl, 150 mM NaCl) containing 0.01% Tween (TBS-Tween) during 30 min at room temperature, for apoAI or apoAII respectively. After 3 washes with TBS-Tween, the membrane was incubated at 4 °C overnight with goat anti-human apoAI (1:10000) or anti-human apoAII (1:1000) antibodies. The blot was then washed 3 times with TBS-Tween. Detection of the antibody−apolipoprotein complexes was performed using a rabbit anti-goat antibody linked to horseradish peroxidase (1:10000) incubated for 1 h. After 3 washes with TBS-Tween and one with TBS, apolipoproteins were visualized by enhanced chemiluminescence.

Determination of α-Tocopherol and β-Carotene Contents of HDL_3 and LDL. The simultaneous determination of αTocOH and β-carotene was carried out by reverse phase HPLC using a method derived from several published reports (*15*−*17*). Aliquots of 250 μL of LDL (∼2 mg of proteins) or HDL_3 (∼1.5 mg of proteins) were added to 1 mL of methanol, 250 μL of distilled water, and 25 μL of 1 mM α-tocopherol acetate and then vigorously shaken for 30 s. After addition of hexane (2 mL), the solution was vortex-mixed for 1 min and then centrifuged during 10 min at 4500 rpm. After centrifugation, 1.5 mL of the supernatant was evaporated to dryness under nitrogen. Before HPLC measurement, the dry extract was dissolved in 250 μL of an ethanol/dichloroethane mixture (4:1, v/v). Reverse phase HPLC was carried out with a Bondapak C18/Corasil pre-

column (30−50 μm, 2.3 cm × 0.39 cm) and a μBondapak (10 μm, 15 cm × 0.39 cm) provided by Waters. A gradient of two mobile phases (20 min, flow rate: 1 mL/min) was used for elution. Phase A was a mixture of water/acetonitrile/methanol (30:50:20, v/v/v) and phase B a mixture of acetonitrile/methanol/ethanol/dichloroethane (10:10:50:30, v/v/v/v). Absorbances were monitored at 292 nm ($\epsilon = 4070$ M^{-1} cm^{-1}) and at 452 nm ($\epsilon = 137\,400$ M^{-1} cm^{-1}) to detect αTocOH and β-carotene, respectively.

Pulse Radiolysis. The pulse radiolysis system used for kinetic measurements on time scales up to 3−4 ms has been previously described (*18*, *19*). For longer time scales (up to 1 min) the conventional detection system is replaced by an OLIS double-beam rapid scan spectrophotometer which facilitates simultaneous kinetic and spectral measurements. In all experiments, a Corning O-52 optical filter, which removes all wavelengths shorter than 330 nm, was placed in the analyzing light beam preceding the sample cell to avoid apolipoprotein and αTocOH photo-oxidation (*20*). Radical concentrations, calculated from transient absorption data, are referenced to $^{\bullet}(SCN)_2^-$ dosimetry (*21*). Radiolytic yield is generally expressed by its *G* value, i.e., the number of radicals generated per 100 eV of absorbed energy. However, such yields, normally expressed in units of grays, may be recast as radical concentrations per unit radiation dose (e.g., a *G* value of 6.13 corresponds to a concentration of 0.63 μM kg/J or 0.63 μM/Gy). As a convenience for the general reader, *G* values are expressed hereafter in units of μM/Gy.

Solutions for pulse radiolysis were prepared in 10 mM, pH 7, phosphate buffer and saturated with pure N_2O or O_2 as desired. All solutions contained 0.1 M Br^-, a concentration sufficient to ensure that essentially all $^{\bullet}OH$ are converted to $^{\bullet}Br_2^-$. To avoid lipoprotein denaturation, small volumes (up to 15 mL) of the buffer were first bubbled for 15 min with either pure N_2O or O_2, then an aliquot (<1−2 mL) of the dialyzed stock lipoprotein solution was added under anaerobic conditions to the N_2O- or O_2-saturated buffer, and the resulting lipoprotein solution was further slowly bubbled with the desired gas during 5 more minutes prior to pulse radiolysis experiments. To minimize the quantity of lipoproteins consumed in each experiment, a microcell (optical path, 1 cm; volume, 400 μL) was used for transient recording. This microcell was emptied and refilled after each shot so that all data were obtained with un-irradiated lipoprotein solutions. Numerical integrations, for analyses of rate data, were carried out using OriginPro software from NAG Software Partners or Scientist software from Micromath Scientific Software. For the convenience of general readers—and as appears in figures showing kinetics data from competitive reactions occurring from short to long time scales—the pseudostationary state approximation was used whenever possible for the determination of first-order rate constants. Rate constants and their uncertainty have been determined from raw data by the calculations with above software and show the precision of curve fitting.

Steady State γ-Irradiations. The γ-radiolysis experiments were carried out with the IBL 637 irradiator (CIS-Bio International, Gif-sur-Yvette, France) equipped with four ^{137}Cs sources delivering up to 54 Gy/min and located at the "Institut Curie" in Paris. Solutions of HDL_3 containing 0.42 mg of protein/mL (~5.2 μM) were prepared in 10 mM, pH 7, phosphate buffer containing 50 μM EDTA and 0.1 M KBr. Under such conditions, more than 99% of $^{\bullet}OH$ radicals generated radiolytically are scavenged by excess Br^- to produce $^{\bullet}Br_2^-$ (*11*). The presence of EDTA during and after the irradiation prevented the initiation of radical chain peroxidation of lipid by redox metal ion contamination. Glass vials containing 1 mL of HDL_3 solution were gently bubbled through septa with air or pure N_2O, and were γ-irradiated with 0, 5, 10, or 20 Gy at a dose rate of 3.95 Gy/min. Irradiated samples were immediately frozen at −80 °C and kept at this temperature until Western blotting and fluorescence measurements could be carried out.

Fluorometric Determination of Intact Trp and Bityrosine Formation in HDL_3. The determination of intact Trp in HDL_3 fractions was performed on denatured HDL_3 as earlier described (*22*). Fifty microliters of the γ-irradiated HDL_3 solution were diluted with 950 μL of 1% *N*-cetyl-*N*,*N*,*N*-trimethyl-ammonium bromide in 50 mM, pH 7, phosphate buffer. The Trp fluorescence was excited with 294 ± 3 nm light which is specifically absorbed by Trp residues and was recorded in the 300−450 nm range or was directly measured at 340 ± 3 nm corresponding to the emission maximum of Trp under these conditions. Bityrosine fluorescence was recorded with the same solution as that used for Trp determination, but the emission was scanned from 350 to 500 nm under excitation at 328 ± 5 nm. To enhance fluorescence yield, the emission was also measured with 1% *N*-cetyl-*N*,*N*,*N*-trimethyl-ammonium bromide in 50 mM, pH 9, borate buffer (*7*).

RESULTS

One-Electron Oxidation of HDL_3 and LDL Apolipoproteins by $^{\bullet}Br_2^-$ Radical-Anions in N_2O-Saturated Solutions. In addition to H_2O_2, several primary radical species are formed by the deposition in oxygen-free water of high-energy ionizing radiation such as high-energy electrons, γ rays, or X-rays. The species formed are hydrated electrons (e_{aq}), hydrogen atoms ($H^{\bullet}$), and hydroxyl radicals ($^{\bullet}OH$). Their formation can be summarized by

$$H_2O \rightsquigarrow e_{aq}, H^{\bullet}, {}^{\bullet}OH, H_2O_2$$

All these species react with a large variety of organic and inorganic molecules. Hydrated electrons (e_{aq}), the strongest reducing species known, can be conveniently transformed into the strongest oxidant $^{\bullet}OH$ radical ($E_0(^{\bullet}OH,H^+/H_2O) = 2.73$ V) by saturating the aqueous solution with N_2O which transforms e_{aq} into $^{\bullet}OH$ radicals according to the reaction

$$e_{aq} + N_2O \rightarrow {}^{\bullet}OH + N_2 + OH^- \quad (1)$$

Because of this highest redox potential, the $^{\bullet}OH$ radical is not specific in its reactivity with proteins and can attack a variety of sites on proteins. This behavior makes it difficult to determine which reactions are biologically relevant. Clearly more specific reactions are required to selectively oxidize specific amino acids. Classical methods used in the radiation chemistry of enzymes for the identification of key residues involve the use of radicals that attack specific functional amino acids. Certain inorganic free radicals have such properties. One widely used species is the dibromine radical-anion, e.g., $^{\bullet}Br_2^-$ formed by the reaction

$$^{\bullet}OH + 2Br^{-} \rightarrow {}^{\bullet}Br_2^{-} + OH^{-} \quad (2)$$

In pulse radiolysis of N_2O-saturated solutions, $^{\bullet}Br_2^{-}$ radical-anion is produced with a yield $G = 6.2$ (0.64 μM/Gy) and, in the absence of proteins, decays with a rate constant of $2k_3 = 4.3 \times 10^9$ M^{-1} s^{-1} (*23*) by the recombination reaction:

$$^{\bullet}Br_2^{-} + {}^{\bullet}Br_2^{-} \rightarrow \text{products} \quad (3)$$

The lower redox potential of $^{\bullet}Br_2^{-}$ ($E_0(^{\bullet}Br_2^{-}/2Br^{-}) = 1.63$ V) compared to that of $^{\bullet}OH$ leads to much greater selectivity in its reactions with amino acid residues. At pH 7, its reactivity toward Trp is about 5 times that of Cys, 30 times that of Tyr, and about an order of magnitude greater than that of His and Met (*11*). The one-electron oxidation of apolipoprotein residues by $^{\bullet}Br_2^{-}$ occurs according to the reaction illustrated in reaction 4 with apoAI, although this scheme is equally applicable to other apolipoproteins.

$$^{\bullet}Br_2^{-} + \text{apoAI} \rightarrow {}^{\bullet}\text{apoAI} + 2Br^{-} \quad (4)$$

As reaction 4 is in competition with reaction 3, it is necessary to design experiments carefully with regard to concentrations of apoprotein and radical.

While all human HDL_3 particles contain 2 molecules of apoAI, about 75% of them also contain 2 molecules of apoAII (*14*). Each apoAI contains 4 Trp, 7 Tyr, 4 His, and 4 Met (*24*), whereas each apoAII contains 4 Tyr and 1 Met (*25*) as potential targets of the $^{\bullet}Br_2^{-}$ reaction. By contrast, the apoB of LDL is characterized by the presence of 37 Trp, 9 free Cys, and 151 Tyr.

The transient absorption spectra of proteins in the near-UV and visible regions immediately after $^{\bullet}Br_2^{-}$ oxidation are due to the presence of $TyrO^{\bullet}$ and $^{\bullet}Trp$ (*11*, *26*, *27*) (Figure 1). In protein environments, these radicals exhibit transient absorbance with maxima at 410 nm ($\epsilon = 2700$ M^{-1} cm^{-1}) and 520 nm ($\epsilon = 1750$ M^{-1} cm^{-1}) for $TyrO^{\bullet}$ and $^{\bullet}Trp$, respectively (*26*). There is negligible contribution of the $TyrO^{\bullet}$ radical absorption at 520 nm, and $^{\bullet}Trp$ radical absorption at 410 nm is reduced to 300 M^{-1} cm^{-1} (*26*). Accordingly, $TyrO^{\bullet}$ and $^{\bullet}Trp$ transient species are readily observed in Figure 1A, which shows transient absorbance spectra of HDL_3 recorded at various times after $^{\bullet}Br_2^{-}$ oxidation of 12.5 μM HDL_3. It may be seen that the transient spectrum of isolated apoAII, which lacks Trp residues, exhibits no absorbance beyond 500 nm (Figure 1A). In HDL_3, growth of $^{\bullet}Trp$ at 520 nm is observed within ~50 μs of the radiolytic pulse. Figure 2A demonstrates that $^{\bullet}Br_2^{-}$ oxidation of apoAI and apoAII in HDL_3 is fast, with a reaction rate constant k_4 of 1.7×10^9 M^{-1} s^{-1}. In LDL, the higher Trp and Tyr content accounts for the faster reaction rate constant (1.1×10^{10} M^{-1} s^{-1}) for the oxidation of apoB by $^{\bullet}Br_2^{-}$ (*23*). Under our dose conditions (i.e., ~8 Gy), pseudo-first-order kinetics apply to the 520 nm absorbance growth in competition with reaction 4 because of the large excess concentration of reactive residues (>500 μM) as potential targets of the ~5 μM $^{\bullet}Br_2^{-}$. The competing second-order decay of $^{\bullet}Br_2^{-}$ was taken into account for these calculations. The $^{\bullet}Trp$ yield in HDL_3 determined from the maximal absorbance at 520 nm is found to be 0.2 μM/Gy (Table 1). This yield corresponds to oxidation involving 4 Trp of the apoAI, as estimated from the yield obtained from

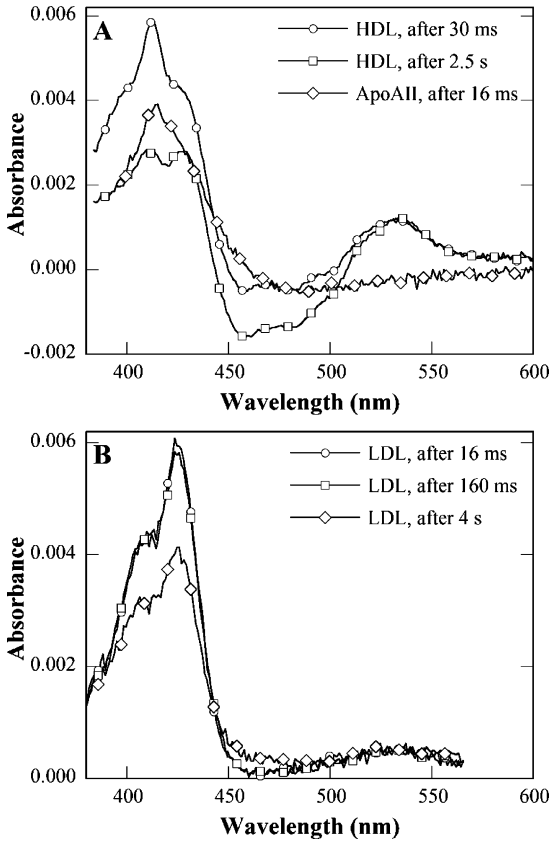

FIGURE 1: Absorbance of apolipoprotein radicals in HDL_3, apoAII, and LDL. (A) Transient absorbance spectra of 12.5 μM HDL_3 (○, □) and 20 μM apoAII (◇) in N_2O-saturated 10 mM, pH 7, phosphate buffer recorded 16 ms (◇), 30 ms (○), and 2.5 s (□) after oxidation with $^{\bullet}Br_2^{-}$ radical-anions. Radiolytic doses were 5.1 Gy and 4.5 Gy for HDL_3 and apoAII, respectively. (B) Transient absorbance spectra of 1.6 μM LDL in N_2O-saturated 10 mM, pH 7, phosphate buffer recorded 16 ms (○), 160 ms (□), and 4 s (◇) after oxidation with $^{\bullet}Br_2^{-}$ radical-anions. Radiolytic dose was 6.2 Gy.

$^{\bullet}Br_2^{-}$ oxidation in 100 μM of Trp in the free form in buffer, i.e., a concentration equivalent to that of the 8 Trp residues of the two apoAI in 12.5 μM HDL_3. Under these conditions, the $G(^{\bullet}Trp)$ for Trp in the free form is 0.45 μM/Gy, somewhat below the potential value of 0.64 μM/Gy for complete conversion of $^{\bullet}Br_2^{-}$ to $^{\bullet}Trp$. This is expected at low Trp concentration because of competition with the fast decay of $^{\bullet}Br_2^{-}$ (reaction 3) (*23*).

As also observed with the transient spectra in Figure 1A, most HDL_3 ($^{\bullet}Trp$) radicals disappear within 1 ms but a small fraction (~ 25%), possibly representing one oxidized Trp (Figure 2B), exhibits a duration of several seconds. The lower limit of the $TyrO^{\bullet}$ yield given in Table 1 (0.3 μM/Gy) has been obtained about 250 μs after the radiolytic pulse from the absorbance decay at 410 nm when the contribution of the strong absorbance of the $^{\bullet}Br_2^{-}$ species becomes negligible (see also ref 23). When the oxidation is carried out with 20 μM apoAI or apoAII in the free form, the total $^{\bullet}Trp + TyrO^{\bullet}$ yield approaches 0.5, i.e., somewhat in excess of the value found for native HDL_3. It can therefore be concluded that Tyr and Trp residues are essentially the only initial targets of HDL_3 oxidation by $^{\bullet}Br_2^{-}$.

Repair of HDL_3 and LDL Phenoxyl Radicals by Plasma α-Tocopherol. Time-dependent changes in the transient spectrum for Tyr and Trp residues of HDL_3 after one-electron

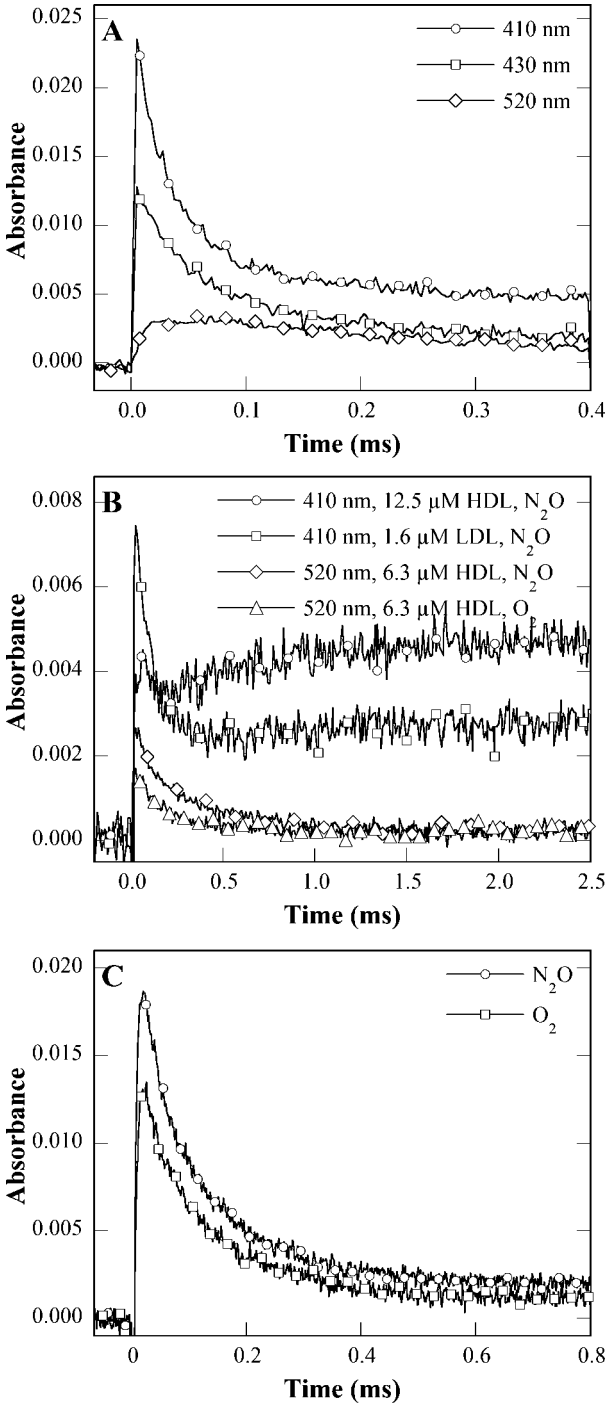

FIGURE 2: Kinetics of radical decays in HDL_3 and LDL. (A) Decay of transient absorbance at 410 nm (○), 430 nm (□), and 520 nm (◇) after pulse radiolysis of 12.5 μM HDL_3 in N_2O-saturated 10 mM, pH 7, phosphate buffer containing 0.1 M KBr. Radiolytic doses were 4.8 Gy for decays at 410 and 430 nm and 8.2 Gy at 520 nm. (B) Decay of transient absorbance at 410 nm after pulse radiolysis of N_2O-saturated 10 mM, pH 7, phosphate buffer containing 0.1 M KBr in the presence of 12.5 μM HDL_3 (○) and 1.6 μM LDL (□) (dose: 4.9 Gy in both cases). Corresponding decays measured at 520 nm with 6.3 μM HDL_3 solutions saturated with N_2O (◇) and O_2 (△). Dose was 4 Gy in both cases. (C) Decay of transient absorbance at 410 nm after pulse radiolysis of 0.8 μM LDL solutions in 10 mM, pH 7, phosphate buffer containing 0.1 M KBr saturated with N_2O (○) or O_2 (□). Radiolytic doses were 4.8 Gy (N_2O) and 6.4 Gy (O_2).

oxidation are clearly observed in Figure 1A. The initial spectrum shows absorbance maxima at 410 nm and at 520 nm that are characteristic of TyrO• and •Trp radicals, respectively. The shoulder initially present at 430 nm evolves at longer times into an absorbance maximum at 430 nm. A similar maximum at 430 nm is observed in LDL only 16 ms after the pulse (Figure 1B). It is most probable that this absorbance at 430 nm originates from an endogenous component common to both HDL_3 and LDL. It is known that these lipoproteins are the blood carriers of αTocOH, and it is well-established that one-electron oxidation of αTocOH leads to the formation of the αTocO• radical whose characteristic absorption maximum is at 430 nm ($\epsilon = 7100$ M^{-1} cm^{-1}) with a shoulder at 410 nm ($\epsilon = 4500$ M^{-1} cm^{-1}) (*28*−*30*). Hence, we attribute the 430 nm transient to αTocO• resulting from oxidation of αTocOH by oxidized apoAI and apoAII of HDL_3 or from oxidized apoB of LDL according to

$$\alpha\text{TocOH} + {}^{\bullet}\text{apoAI, }{}^{\bullet}\text{apoAII (or }{}^{\bullet}\text{apoB)} \rightarrow \alpha\text{TocO}^{\bullet} + \text{apoAI, apoAII (or apoB)} \quad (5)$$

In LDL, after an initial fast decay of the TyrO• transient at 410 nm, a plateau in αTocO• absorption is observed at 410 nm (Figure 2B). This observation, coupled with the formation of a long-lived Trp radical whose absorbance still persists 4 s after the oxidation with $^{\bullet}Br_2^-$ (see Figure 1B), suggests that the only precursor of the αTocO• radical is the TyrO• radical. Indeed, the decay of the TyrO• radical appears to be a monomolecular process with the rate constant $k_5 = (1.25 \pm 0.05) \times 10^4$ s^{-1}. This kinetic behavior is independent of radiolytic dose and LDL concentration (data not shown). It suggests the occurrence of an intramolecular reaction, since αTocOH is most likely solubilized in the surface phospholipid monolayer of the lipoprotein carriers (*31*) and hence not readily accessible to bimolecular reactions resulting from collision between oxidized LDL particles in the bulk. In the case of HDL_3, by contrast, a fast initial decay is observed at both 410 and 430 nm over about 200 μs (Figure 2A), followed by the growth of the αTocO• transient over several milliseconds as illustrated by Figure 2B at 410 nm, a wavelength also corresponding to the shoulder of the αTocO• transient where the molar absorbance is 4500 M^{-1} cm^{-1}. This second step thus occurs over a much slower time scale (Figure 2B) and is in agreement with time-dependent spectral changes observed in Figure 1A.

Figure 2A demonstrates that there is negligible oxidation of αTocOH by $^{\bullet}Br_2^-$ since the absorbance ratio $A_{410\text{ nm}}/A_{430\text{ nm}}$ after 400 μs is 2.2 in reasonable agreement with that for TyrO• (*26*, *27*) but not with that for the αTocO• radical, which exhibits a value of 0.6. The rate constant of the slow first order αTocO• growth is $k_5 = (1.4 \pm 0.2) \times 10^3$ s^{-1}, notably slower than the decay of the Trp• transient at 520 nm which gives a rate constant of $(2.6 \pm 0.3) \times 10^3$ s^{-1}. The initial yields of the αTocO• radical produced are reported

Table 1: One-Electron Oxidation Yields of ApoAI and ApoAII in the Free Form and of HDL_3 by the Selective $^{\bullet}Br_2^-$ Radical-Anions[a]

radical	apoAI	apoAII	HDL_3
TyrO•	0.16[b]	0.48	0.30
•Trp	0.31	*c*	0.20

[a] Experiments were carried out at 20 °C with 20 μM apoAI or apoAII or with 12.5 μM HDL_3 in N_2O-saturated 10 mM, pH 7, phosphate buffer containing 0.1 M Br^-. Dose was 4.5 Gy. [b] Yields are expressed in μM/Gy. [c] ApoAII has no Trp residues.

Table 2: Initial Yields (G) and Rate Constants of Decay (k) of the α-Tocopheroxyl Radical (αTocO•) in LDL and HDL_3[a]

	HDL_3		LDL	
parameter	N_2O	O_2	N_2O	O_2
G[b] (μM/Gy)	0.18	0.10	0.12	0.07
k (s^{-1})	9.5 ± 0.6	49.8 ± 0.8	5.8 ± 0.5	24.3 ± 0.9
	1.5 ± 0.1	3.3 ± 0.2	0.8 ± 0.1	2.1 ± 0.2

[a] Experiments were carried out at 20 °C with 12.5 μM HDL_3 or 1.6 μM LDL in N_2O or O_2-saturated 10 mM, pH 7, phosphate buffer containing 0.1 M Br^-. Dose was 4.8 Gy. [b] Data are initial values, i.e., determined ~3 ms after the pulse (see Figure 3A) from the transient absorbance at 430 nm using $\epsilon = 7100\ M^{-1}\ cm^{-1}$ for the αTocO• radical.

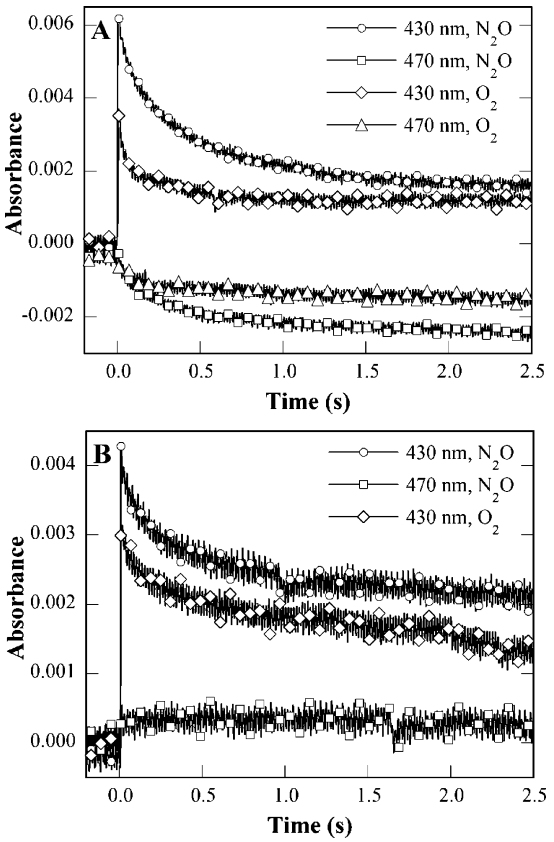

FIGURE 3: Kinetics of repair of semioxidized αTocOH by carotenoids. (A) Decay of αTocO• radical absorbance at 430 nm (○, ◇) and bleaching of Car absorbance at 470 nm (□, △) after oxidation of 12.5 μM HDL_3 by $^{\bullet}Br_2^-$ radical-anions in 10 mM, pH 7, phosphate buffer. Solutions were saturated with N_2O (□, ○) and O_2 (◇, △). Radiolytic doses were 4.8 Gy for N_2O-saturated solutions and 7 Gy for O_2-saturated solutions. (B) Corresponding transient absorbance changes measured at 430 nm (○, ◇) and 470 nm (□) for solutions containing 1.6 μM LDL. Doses were 4.8 Gy for N_2O-saturated solutions (○, □) and 7 Gy for O_2-saturated solutions (◇).

in Table 2 and have been determined from data such as those shown in Figure 3A. Comparison of values in Tables 1 and 2 demonstrates only partial repair of the oxidative damage to apolipoproteins of HDL_3 by endogenous αTocOH. The partial repair of oxidative damage to HDL_3 and LDL is consistent with spectral data, since the TyrO• and/or the $^{\bullet}$Trp transient species are still observed in spectra recorded several seconds after the repair reaction described by reaction 5 (Figure 1A,B). According to HPLC data in Table 3, the αTocOH content in native LDL is ~4 molecules per particle, whereas it drops to about 10-fold in HDL_3. By combining

Table 3: Concentration of Vitamin E and β-Carotene in Native HDL_3 and LDL Fractions Isolated from Human Plasma by Sequential Ultracentrifugation and Used for Pulse Radiolysis Experiments[a]

antioxidant (μM)	HDL_3	LDL
vitamin E	24.1 (0.31)[b]	57.8 (3.78)[b]
β-carotene	0.19 (0.0024)[b]	1.7 (0.11)[b]

[a] Concentrations were determined by HPLC after extraction as detailed in the experimental section. HDL_3 and LDL concentrations were 6.25 mg/mL (78.1 μM) and 7.65 mg/mL (15.3 μM), respectively. [b] Data in parentheses are the molar ratios (molecules/particle).

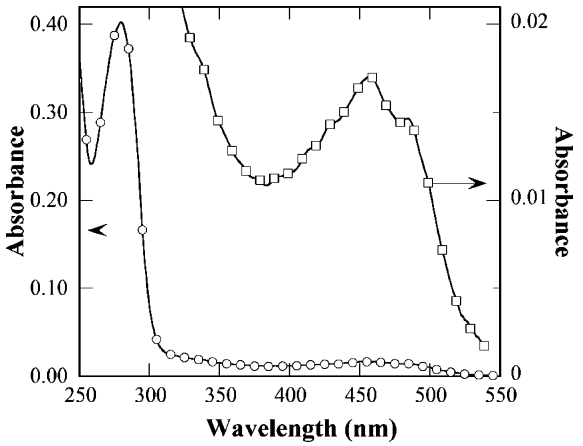

FIGURE 4: Carotenoid absorbance spectrum in HDL. Absorbance spectrum of a 10 mM, pH 7, phosphate buffer solution containing 6.3 μM HDL_3 recorded at two absorbance scales in a 1 cm light-path cuvette at 25 °C. The right ordinate (□) magnifies the absorbance of the Car of the same sample.

data of Tables 2 and 3, it can be concluded, with radiolytic doses (4.8 Gy) and lipoprotein concentrations used in these experiments, that ~22% and 10% of the αTocOH content were oxidized in the HDL_3 and LDL particles, respectively.

Fate of the α-Tocopheroxyl Radical and Its Relationship to Carotenoid Bleaching. Kinetic studies reveal that αTocO• radical decay in HDL_3 (Figure 3A) and LDL (Figure 3B) is a multistep process characterized by a fast and a slow component. Thus, more than 60% of the αTocO• transient in HDL_3 and about 50% in LDL decay within 2.5 s while the remainder decays over more than 1 min as can be estimated from the kinetic traces recorded at 430 nm on Figures 3A and 3B. This slow decay is presumably due to bimolecular dimerization and/or disproportionation (*29*) or to reactions with apolipoprotein radicals. Kinetics corresponding to the fast portion of the αTocO• radical decay in HDL_3 and LDL are well fitted by two parallel first-order reactions, decays being twice as fast in HDL_3 as in LDL (Table 2). In HDL_3, the extent of the fast decay corresponds to about half of the radicals generated (Table 2).

From comparison of Figures 1A and 1B, the major difference observed between HDL_3 and LDL is the bleaching of HDL_3 absorbance in the 450−485 nm region where endogenous Car constitute the only absorbing species (Figure 4). This is a striking but paradoxical result since LDL contains approximately 10 times more Car than HDL_3 according to data in Table 3. Here, β-carotene may be taken as an indicator of the total Car content, as it represents about 20% of major plasma Car (*15*). The time-dependent bleaching of the Car has been followed at 470 nm (Figure 3A), at

which wavelength αTocO• transient absorbance ($\epsilon_{470\ nm} \sim 1200\ M^{-1}\ cm^{-1}$) is minimal. It can be seen that the time scale of the bleaching parallels that of the αTocO• transient decay.

LDL and HDL_3 are natural carriers of Car in plasma, and it has been previously established that, in hexane, the αTocO• radical can be reduced by lutein, cathaxanthin, β-carotene, lycopene, and other Car at diffusion controlled rates (*32*, *33*). Here, one-electron oxidation of the Car leads to repair of αTocO• and permanent bleaching (i.e., destruction) of Car via formation of the Car radical-cation according to the reaction

$$\alpha TocO^{\bullet} + Car \rightarrow {}^{\bullet}Car^{+} + \alpha TocOH \qquad (6)$$

As with αTocO• decay, Car bleaching can be explained by two parallel first-order reactions with k_6 values of 9.0 ± 0.7 and 1.03 ± 0.05 s^{-1}, respectively. These are consistent with the rate constants obtained for the disappearance of the αTocO• radicals (Table 2).

An estimate of the repair yield of the αTocO• radicals by endogenous Car, 3 s after the onset of the HDL_3 oxidation by $^{\bullet}Br_2^{-}$, can also be obtained from Figure 3A data. The Car bleaching yield can be determined assuming an average molar absorbance of 110 000 $M^{-1}\ cm^{-1}$ at 470 nm. This molar absorbance value has been chosen since the $A_{450\ nm}/A_{470\ nm}$ absorbance ratio in the HDL_3 spectrum is 1.15 (Figure 4), and the average molar absorbance of Car at 448 nm is 140 000 $M^{-1}\ cm^{-1}$. This yield has been determined by taking into account the molar absorbance and the relative proportion—on a molar basis—of major Car in plasma (*17*). With these values, the bleaching yield is found to be 0.004 μM/Gy corresponding to only 2% that of the initial αTocO• radicals. Incidentally, it should be noted that this average molar absorbance and the β-carotene content in Table 3 may be used to estimate a value of 7 for the ratio [Car]/[β-carotene] in fair agreement with literature data (*15*).

Sensitivity of the α-Tocopheroxyl Radical Decay and Carotenoid Bleaching to the Presence of O_2. The effect of oxygen on radical reactions involved in the formation and repair of oxidative damage in apoAI and apoAII or in apoB has been investigated because of its obvious relevance to oxidation occurring *in vivo*. While literature data indicate that •Trp, TyrO•, and αTocO• are rather unreactive with oxygen, •Trp, in the free form or in proteins (*34*, *35*), as well as αTocO• (*36*) and TyrO• (*37*) readily react with the $^{\bullet}O_2^{-}$ at nearly diffusion controlled rates. On the other hand, the $^{\bullet}O_2^{-}$ radical-anion can directly oxidize Car (*32*) but not Trp (*35*) or αTocOH (*30*). However, it can be anticipated that the complex lipoprotein structure and associated microenvironments may affect the reactivity of $^{\bullet}O_2^{-}$ with the above species.

Pulse radiolysis of an O_2-saturated solution containing 0.1 M Br^{-} produces $^{\bullet}O_2^{-}$ with a radiolytic yield $G = 0.34$ μM/Gy by the following reactions:

$$e_{aq}^{-} + O_2 \rightarrow {}^{\bullet}O_2^{-} \qquad (7)$$

$$H^{\bullet} + O_2 \rightarrow {}^{\bullet}O_2^{-} + H^{+} \qquad (8)$$

The radiolytic yield of $^{\bullet}Br_2^{-}$ radicals formed under these conditions is thus reduced to 0.32 μM/Gy since reaction 1 does not occur in this system. Consequently, as exemplified with HDL_3, the •Trp radical yield in Figure 2B is reduced in O_2-saturated solutions to about half that produced by N_2O-saturation with the same irradiation dose (i.e., 4 Gy). As apparent from this figure, •Trp decay (rate constant: 2.4 ± 0.1 s^{-1}) is insensitive to the presence of $^{\bullet}O_2^{-}$. A similar lack of reactivity was observed with LDL (data not shown) suggesting inaccessibility of oxidized Trp residues to $^{\bullet}O_2^{-}$ in both lipoproteins. Similarly, as shown in Figure 2C, no reaction was observed with TyrO• in the case of LDL.

As expected, the αTocO• radical yields in Table 2, resulting from the repair of the oxidative damage on apoAI and apoAII as well as on apoB, are about half those measured under N_2O. On the other hand, at short times after the pulse, the initial rate of αTocO• radical decay increases while the slow portion, representing at least 50% of the absorbance, is hardly affected by the presence of $^{\bullet}O_2^{-}$ (Figure 3A,B). Thus, three categories of αTocO• species appear to be present in the lipoproteins. However, only two of them react with $^{\bullet}O_2^{-}$, via

$$\alpha TocO^{\bullet} + {}^{\bullet}O_2^{-} + H^{+} \rightarrow \alpha TocOH + O_2 \qquad (9)$$

to partially restore αTocOH. In HDL_3 and LDL, this reaction can be considered as pseudo first order since there is an approximately 5-fold $^{\bullet}O_2^{-}$ excess concentration produced by the radiolytic pulse, i.e., 0.34 μM/Gy as compared to the concentration of reactive αTocO•. An estimate of k_9 may be made using the rate constants given in Table 2 determined in the presence or absence of oxygen, through Stern−Volmer type kinetic analysis. In this manner, for HDL_3 a rate constant k_9 equal to $\sim 2.5 \times 10^7\ M^{-1}\ s^{-1}$ is determined from the rate constants 49.8 and 9.5 s^{-1} in the presence and absence of oxygen respectively (see Table 2). Similarly for LDL, a rate constant k_9 equal to $\sim 1.1 \times 10^7\ M^{-1}\ s^{-1}$ can be estimated. When these calculations are carried out with the αTocO• species reacting with $^{\bullet}O_2^{-}$ at long time, i.e., with rate constants of 3.3 and 2.1 s^{-1} for HDL_3 and LDL respectively in the presence of oxygen (see Table 2), the corresponding k_9 values approach the same value, i.e., $\sim 1 \times 10^6\ M^{-1}\ s^{-1}$.

As can be seen in Figure 3A, a small yield (~0.002 μM/Gy) of Car bleaching is still observed with HDL_3 under O_2 saturation. In HDL_3, this behavior is explained by repair of αTocO• radicals through competing reactions 6 and 9. The absence of Car bleaching in LDL rules out direct Car oxidation by $^{\bullet}O_2^{-}$.

Permanent Damage Associated with the Incomplete Repair of Radical Damage to ApoAI in HDL_3. Changes in ApoAI and ApoAII Gel Migration and Trp Content. The β-carotene and αTocOH contents in the HDL_3 fractions prepared for these experiments, i.e., 0.0024 and 0.34 molecule per particle respectively, were close to those used for pulse radiolysis. Furthermore, it may be noted that the primary reactive species produced during steady state γ-radiolysis of aqueous solutions are the same as those formed during pulse radiolysis with accelerated electrons. Therefore reactions 1−4, 7, and 8 also apply to this system. After γ-irradiation with doses of 5, 10, or 20 Gy, N_2O- or air-saturated HDL_3 solutions were subjected to 12% SDS−polyacrylamide gel electrophoresis under reducing and nonreducing conditions. Coomassie Blue staining was performed to check the integrity of HDL_3 samples (data not shown). Parallel Western blots,

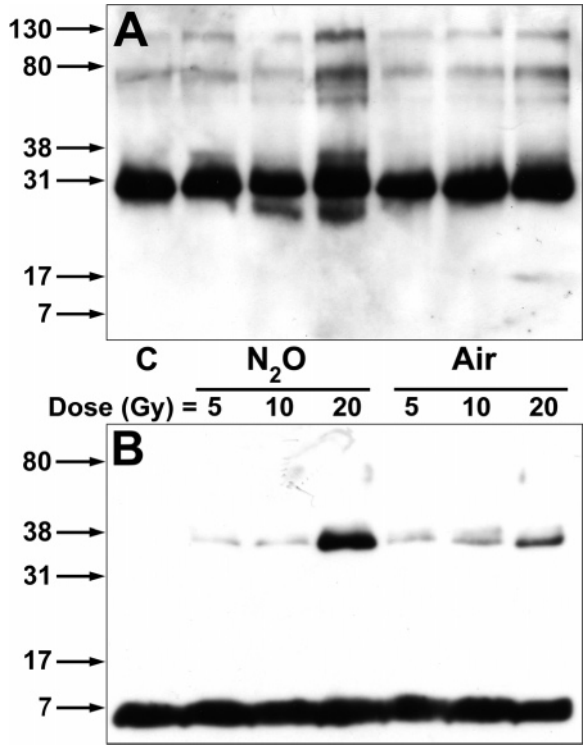

FIGURE 5: Modifications of apoAI and apoAII of γ-irradiated HDL_3. Unirradiated (controls, "C") and N_2O- or air-saturated HDL_3 samples irradiated with 5, 10, and 20 Gy were subjected to 12% SDS−polyacrylamide gel electrophoresis and transferred to nitrocellulose membrane for immunoblotting. The immunoblots were probed with goat anti-human apoAI antibody in nonreducing conditions (A) or with goat anti-human apoAII antibody in reducing conditions (B). Molecular weight markers are indicated.

performed on separate gels, were probed with anti-human apoAI or apoAII antibodies (Figure 5). No major difference was observed under reducing and nonreducing conditions except that apoAII migrated as a monomer or as a dimer, respectively. More pronounced effects were generally observed after irradiation of N_2O-saturated samples, consistent with the 2-fold increase in the radiolytic yield of $^{\bullet}Br_2^-$. Western blot in Figure 5A shows that irradiation under N_2O or air leads to dose-dependent modifications of apoAI migration with the appearance of diffuse bands flanking the ~28 kDa position of non-irradiated HDL_3. The band at lower molecular weight, mostly observed under N_2O, might represent a small amount of apoAI fragmentation. The band at ~36 kDa was observed with both the anti-apoAI (Figure 5A) and anti-apoAII (Figure 5B) antibodies, therefore suggesting that it is a heterodimer of apoAI cross-linked to an apoAII monomer (*38*). Other bands at ~60, 70, and 130 kDa also appeared on Western blots probing apoAI (Figure 5A), which might correspond to various degrees of covalent polymerization of modified apoAI. However, a weak band at 70 kDa is seen in the control lane of Figure 5A. It may correspond to little amounts of contaminating HSA (*39*) since it is also present when probing the blot with an anti-human HSA antibody.

While no bityrosine fluorescence could be detected, a biphasic loss of Trp in γ-irradiated HDL_3 solution was observed. About 25% of the Trp disappeared after irradiation with 5 Gy in either N_2O- or air-saturated solutions (Figure 6). Subsequently, after a further dose of 15 Gy, an additional 10% Trp loss is recorded. This biphasic behavior suggests

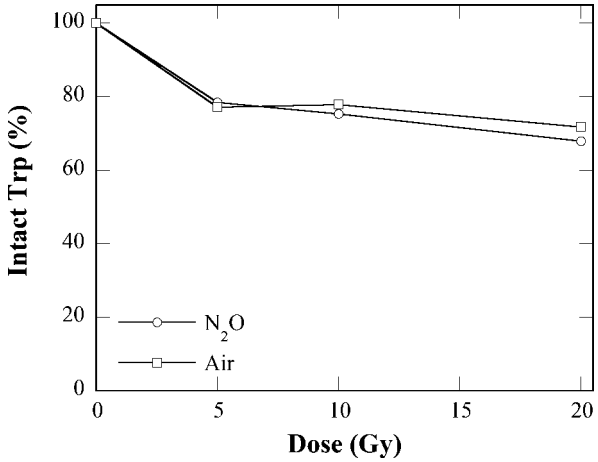

FIGURE 6: Trp loss in γ-irradiated HDL_3. Dose-dependent loss (in percent) in the Trp content of γ-irradiated 10 mM, pH 7, phosphate buffer solutions containing 5.2 μM HDL_3, 50 μM EDTA and 0.1 M KBr. (○) N_2O-saturated solutions; (□) air-saturated solutions. Temperature: 25 °C.

that in native HDL_3 there are two classes of residues among the 8 Trp whose accessibility to oxidation by $^{\bullet}Br_2^-$ radical-anions differs. This observation is consistent with the time-resolved measurements above. However, the lack of oxygen effect on the Trp loss under air saturation, even though the $^{\bullet}Br_2^-$ yield is halved, suggests oxygen-induced secondary reactions inherent to the time scale of steady-state irradiation conditions. For example, lipid peroxidation may contribute to the Trp loss within the apoAI. Additionally, there is an almost 3-fold increase in H_2O_2 formation under air as compared to N_2O saturation which may be involved in processes leading to such loss.

DISCUSSION

The antiatherogenic properties of HDL are compromised by oxidative modification (*40*), and it has been established that such oxidation, via various mechanisms, involves changes in apoAI residues, namely, Trp, Lys, and Tyr (*5*, *8*). Parenthetically, the $^{\bullet}$Trp radical has also been proposed as the initiator of LDL lipid peroxidation induced by Cu^{2+} (*41*). In atherogenesis, the key role played by the MPO of phagocytes is evidenced by the presence of chlorination products of Tyr in human atherosclerotic lesions, and their systemic levels are considered as predictors of atherosclerotic risk (*5*). However, a very recent study (*8*) points to uncertainty regarding the respective roles that oxidation of these residues plays in the impairment of HDL function. Importantly, the nature and number of involved primary chemical intermediates leading to irreversible damage have not been resolved.

This study provides the first account of the sequence of reactions involving radical intermediates in HDL_3 which commences with the selective oxidation of critical aromatic apolipoprotein residues and terminates with the imperfect repair of the protein damage by endogenous antioxidants. These reactions are summarized in the scheme given in Figure 7. Coupled with observations in LDL, the work supports the contention that the oxidation of lipids, observed after treatment of HDL by MPO-related oxidants, may occur as a secondary process which commences with apolipoprotein radical formation (*42*). The similarity of products

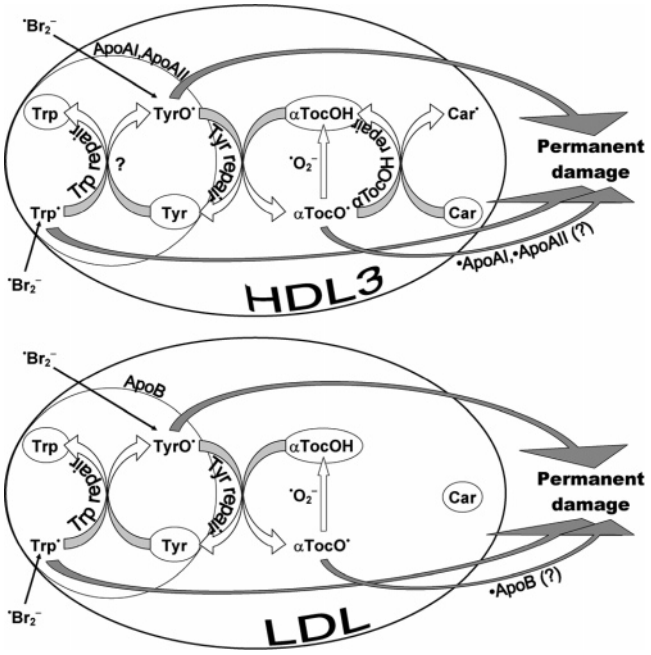

FIGURE 7: Scheme illustrating the sequence of radical reactions beginning with the selective oxidation of Tyr and Trp residues of apoAI and apoAII of HDL and apoB of LDL by $^{\bullet}Br_2^-$ radical-anions followed by the partial repair of the TyrO• by α-tocopherol. Note that in HDL the subsequent repair of the αTocO• by carotenoids can only occur in those particles containing both antioxidants. Radical reactions postulated for the completion of this scheme are indicated by a question mark.

determined following steady-state irradiation of HDL_3 to those found in myeloperoxidase oxidation further supports the contention that mechanisms proposed from this time-resolved study are highly relevant to those operative in *in vivo* oxidative damage (*43*). The key observations of this work are as follows.

The Tyr and Trp Residues Are Selective Targets in the Oxidation of ApoAI by $^{\bullet}Br_2^-$ Radical-Anions. Mild oxidants like $^{\bullet}Br_2^-$, whose redox potential $E_0(^{\bullet}Br_2^-/2Br^-)$ is 1.63 V vs NHE (*44*), react selectively with native LDL (*23*) and HDL (see Table 1), demonstrating that essentially all reacting $^{\bullet}Br_2^-$ are converted into TyrO• and •Trp radicals. Efficient conversion of $^{\bullet}Br_2^-$ into TyrO• and •Trp radicals is also facilitated by the absence of polyunsaturated fatty acid reactivity toward $^{\bullet}Br_2^-$. The relevance of the present findings to MPO mediated oxidation is suggested by the apparently similar accessibility of vulnerable residues to both MPO and $^{\bullet}Br_2^-$ attack. In HDL_3, residues that are targets of MPO include Tyr-29, Tyr-166, Tyr-192, and Tyr-236 (*5*) as well as Trp-8, Trp-72, and Trp-108 (*8*). Although the Trp fluorescence maximum at ~330 nm in native (*22*) or in reconstituted HDL particles with two apoAI (*45*) suggests that Trp residues are not fully exposed to water where the maximum lies at 353 nm, fluorescence quenching experiments show that in reconstituted HDL particles 60% of the fluorescence is quenched by—and thus accessible to—I^- anions. This is consistent with our finding that 4 Trp residues of apoAI are susceptible to oxidation by $^{\bullet}Br_2^-$ radical-anions. Similarly, the Tyr residues of apoAI have been shown to be accessible to reaction with TyrO• radicals formed in buffer by oxidation of excess Tyr with peroxidase (*7*). There is also a contribution from apoAII Tyr residues in the HDL_3 fraction which also contains apoAI. These residues are readily oxidized by $^{\bullet}Br_2^-$ radical-anions in free apoAII (Figure 1A) or apoAI.

A strong case can be made for the formation and reaction of TyrO• and •Trp radicals in physiologically relevant systems. For example, the dihydroxylated Trp oxidation products that are formed in apoAI by the MPO reaction (*8*) have been shown to originate from radicals produced by one-electron oxidation by—or addition of—•OH to the tryptophan indole ring (*9*). Further, the possible formation of bityrosine in oxidized HDL under certain experimental conditions provides additional evidence for TyrO• participation in apoAI oxidation (*7*). While *in vivo* •OH radicals are produced by Fenton-type reactions during the respiratory burst of activated phagocytes to form TyrO• and •Trp radicals by addition/oxidation reactions, it is also likely that the TyrO• and •Trp radicals are produced during oxidation by MPO (*6*). The redox potential of the activated MPO heme−H_2O_2 complex is $E_0 = 1.16$ V at pH 7 (*6*, *46*), i.e., sufficiently high at pH 7 to oxidize Trp (E_0(•Trp,H^+/Trp) ~ 0.98 V) and Tyr (E_0(TyrO•,H^+/Tyr) ~ 0.6 V) (*47*). As well as the destruction of Trp in HDL_3 given in Figure 6, the good correspondence between the Western blots taken following steady γ-irradiation (Figure 5) and those of Peng et al. (*8*) shown in the 15−75 kDa molecular mass range after MPO oxidation of unbound recombinant apoAI is highly consistent with this interpretation.

The Repair of Oxidative Damage to ApoAI and ApoB by α-Tocopherol Is Incomplete. Once formed, the TyrO• and •Trp radicals of apoAI and apoB react over a duration of seconds with αTocOH by an intramolecular one-electron redox process as observed in Figures 1A and 1B. Theoretically, this redox reaction with either TyrO• or •Trp species is feasible since the standard redox potential of the αTocO•,H^+/αTocOH couple is 0.48V at pH 7 (*48*). However, the αTocOH resides predominantly in the phospholipid surface monolayer with the chromanol moiety of αTocOH interacting with the phospholipid headgroups while the phytyl side chain anchors αTocOH in the lipid pseudophase, restricting its mobility (*31*). As explained in Results, the kinetic analyses of TyrO• and •Trp radical decay in LDL clearly suggest that the formation of the αTocO• arises mainly from TyrO• repair, with negligible contribution from •Trp repair. The disappearance of most •Trp radicals by a first-order process may suggest the occurrence of other intramolecular reactions such as the oxidation of intact Tyr residues by •Trp as we previously observed with LDL (*23*). The rest of the •Trp radicals whose transient absorbance is still observed (Figure 1A) seconds after the radiolytic pulse most probably lead to permanent damage of apoB. This behavior strongly indicates a physical inaccessibility of the apoAI •Trp radical to the OH group of αTocOH, the reacting site for reaction with radicals. Thus, full repair of oxidative damage to apolipoproteins by αTocOH is unlikely since the αTocO• radicals are only produced by the repair of TyrO•. In the case of HDL_3, this assumption is in agreement with respective yields of TyrO• and of αTocO• given in Tables 1 and 2. From HPLC data given in Table 3, one may determine that there are ~4 αTocOH molecules per LDL particle but only 1 αTocOH molecule per ~3 HDL particles. This difference has two important consequences. First, there is a much greater intrinsic probability of reaction (4:1) for the repair of TyrO• radicals in those LDL containing αTocOH than in

those HDL particles containing αTocOH. This explains the much faster rates of reaction 5 ($k_5 = (1.25 \pm 0.05) \times 10^4$ s^{-1}) in LDL and the rapid disappearance of the TyrO• radical absorbance over ~300 μs (Figure 1B). Conversely, the persistence of TyrO• radicals in HDL_3 2.5 s after $•Br_2^-$ oxidation is consistent with the absence of αTocOH in 70% of HDL particles (Figure 1A). It is reasonable to conclude that the large fraction of unrepaired TyrO• and •Trp radicals initiates reactions leading to the permanent damage on both apoAI and apoAII shown in the Western blots of Figure 5 and to the oxidation of Trp residues observed by fluorescence (Figure 6).

Repair of the α-Tocopheroxyl Radicals by Carotenoids Occurs, Paradoxically, Only in HDL_3. Both the spectral data from HDL_3 in Figure 1A and the kinetics in Figure 3A provide clear evidence for a bleaching in the absorbance domain characteristic of Car. On the basis of literature spectral data, this bleaching can be attributed to the one-electron oxidation of the Car by αTocO• radicals (see reaction 6), resulting in αTocOH recovery (*32*). In agreement with this assumption, kinetic data demonstrate that the rate constants of Car bleaching parallel those of αTocO• radical decay. Due to the chemical heterogeneity of Car in lipoproteins, the biphasic decay of αTocO• may result from repair by more than one class of Car with differing inherent reactivities (reaction 6, k_6) and/or different accessibilities to αTocO• radicals because of their specific localization in the HDL core. However, in the two thirds of the αTocO• radicals which disappear over the duration of Car bleaching, only a small fraction are actually repaired by Car. Again, as in the case of αTocOH, the distribution of Car molecules among HDL particles may be used to explain the reduced yield of αTocO• repair (0.004 μM/Gy). Calculations made from Figure 4 show that there are 18 times fewer molecules of Car than of αTocOH. As a result, the probability of having one Car molecule and one αTocOH in the same HDL particle, (e.g., the product of individual probabilities) is low. Figure 3A shows that only ~2% of the initially produced αTocO• radicals are repaired by endogenous Car despite the large corresponding disappearance of αTocO•. Thus, competing reactions leading to αTocO• radical destruction, possibly by dimerization and/or disproportionation as well as by reactions with other radical species such as •Trp or other amino acid radicals, would appear to dominate over the repair by Car.

Paradoxically, no Car bleaching is observed in LDL despite the fact that it contains almost 10 times more Car per particle than HDL (Table 3). This result cannot be explained by simple considerations of inherent chemical reactivity. Structural factors are most likely involved which hinder access of Car to αTocO• radicals. It is likely that parts of the apoB are in contact with the lipids in all the three concentric layers of the particle. In LDL particles (diameter: ~20 nm) which are large compared to HDL (diameter: ~9 nm), interpenetration of core lipids (mainly cholesteryl ester, small amounts of triglyceride, and unesterified cholesterol) and phospholipid fatty acid chains has been demonstrated above the transition temperature and in a lesser extent below it by X-ray small-angle scattering (*49*). This interpenetration region probably includes the phospholipid monolayer where αTocOH is localized. By contrast, the long polyenic Car are more likely sequestered within the core. As the present time-resolved experiments were carried out at 24 °C, below the phase transition, the highly ordered cholesteryl ester (*49*) may well produce clusters with strong motional constraints which impede interaction between Car and αTocO• radicals. A different environment may be found in HDL_3. Comparison of LDL and HDL_3 phospholipids by surface pressure measurements on monolayers (*50*) and by electron paramagnetic resonance studies with spin labeled fatty acids (*51*) has demonstrated that the relatively smaller HDL particles, with lower unesterified cholesterol and fewer saturated phospholipids, exhibit a more fluid structure. This increased fluidity and the penetration of apoAI within the particle may well facilitate the full sequence of oxidation and repair reactions observed in HDL_3.

The $•O_2^-$ Radical-Anion Mediates the Antioxidant Response to Oxidative Damage in Apolipoproteins. The respiratory burst of activated neutrophils and mononuclear phagocytes acts as a local chemical reactor in which a large concentration of $•O_2^-$ can be produced. This species can mediate competing reactions pathways of MPO activity as well as participate in reactions of primary chemical intermediates produced by oxidation of plasma constituents, e.g., lipoproteins. The present study identifies three such species which can potentially react with $•O_2^-$, i.e., αTocO• (*36*), •Trp (*34*), and TyrO• (*37*).

The kinetic analyses suggest that, in HDL, only αTocO• radicals accessible to repair by Car can react with $•O_2^-$. Hence, $•O_2^-$ is unreactive toward about half the Car carried by HDL that can react with αTocO• (Figure 3A). As expected, the reaction rate constants, k_9, for repair of αTocO• by $•O_2^-$ in both HDL and LDL are much lower than those reported in organic solvents for freely moving αTocO• radicals (i.e., $\sim 10^9$ M^{-1} s^{-1}) (*29*). This behavior suggests strong motional constraints to $•O_2^-$ diffusion due to the higher viscosity of lipoproteins and to the accessibility of αTocO•. Moreover, these data are consistent with the formation of αTocO• radicals in various microenvironments depending on the interaction of oxidized Tyr residues with the water−lipid interface.

The observation that •Trp and TyrO• radicals formed in apoAI as well as in apoB are insensitive to $•O_2^-$ is also important. With regard to •Trp, this behavior contrasts sharply with previous results involving egg lysozyme, in which 3−4 exposed Trp residues, oxidized by $•Br_2^-$, were readily repaired by $•O_2^-$ radical-anions with a bimolecular rate constant of $\sim 1 \times 10^8$ M^{-1} s^{-1} (*34*). Here, the 7 Trp residues of LDL apoB (*23*) and 4 Trp residues of HDL_3 apoAI oxidized by $•Br_2^-$ appear inaccessible to $•O_2^-$. It is possible that important conformational rearrangements occur in the 500 μs time scale following the oxidation by $•Br_2^-$. Such changes may impede access of $•O_2^-$ to the oxidized residues in contrast to the results of the lysozyme study. Hence, even under aerobic conditions, these long lasting radicals may play a key role in triggering LDL and HDL lipid peroxidation.

ACKNOWLEDGMENT

The authors wish to thank M.-A. Conte for her skillful assistance in the HDL_3 and LDL preparation.

REFERENCES

1. Fielding, C. J., and Fielding, P. E. (1995) Molecular physiology of reverse cholesterol transport, *J. Lipid Res. 36*, 211−228.
2. Parthasarathy, D., Barnett, J., and Fong, P. N. (1990) High-density lipoprotein inhibits the oxidative modification of low-density lipoprotein, *Biochim. Biophys. Acta 1044*, 275−283.
3. Chisolm, G. M., and Steinberg, D. (2000) The oxidative modification hypothesis of atherogenesis: an overview, *Free Radical Biol. Med. 28*, 1815−1826.
4. Babior, B. M. (1978) Oxygen-dependent microbial killing by phagocytes (first of two parts), *N. Engl. J. Med. 298*, 659−668.
5. Zheng, L., Nukuna, B., Brennan, M.-L., Sun, M., Goormastic, M., Settle, M., Schmitt, D., Fu, X., Thomson, L., Fox, P. L., Ischiropoulos, H., Smith, J. D., Kinter, M., and Hazen, S. L. (2004) Apolipoprotein A-I is a selective target for myeloperoxidase-catalyzed oxidation and functional impairment in subjects with cardiovascular disease, *J. Clin. Invest. 114*, 529−541.
6. Ghibaudi, E., and Laurenti, E. (2003) Unraveling the catalytic mechanism of lactoperoxidase and myeloperoxidase, *Eur. J. Biochem. 270*, 4403−4412.
7. Francis, G. A., Mendez, A. J., Bierman, E. L., and Heinecke, J. W. (1993) Oxidative tyrosylation of high density lipoprotein by peroxidase enhances cholesterol removal from cultured fibroblasts and macrophage foam cells, *Proc. Natl. Acad. Sci. U.S.A. 90*, 6631−6635.
8. Peng, D.-Q., Wu, Z., Brubaker, G., Zheng, L., Settle, M., Gross, E., Kinter, M., Hazen, S. L., and Smith, J. D. (2005) Tyrosine modification is not required for myeloperoxidase-induced loss of apolipoprotein A-I functional activities, *J. Biol. Chem. 280*, 33775−33784.
9. Solar, S., Solar, W., and Getoff, N. (1984) Resolved multisite OH-attack on aqueous tryptophan studied by pulse radiolysis, *Radiat. Phys. Chem. 23*, 371−376.
10. Redpath, J. L., Santus, R., Ovadia, J., and Grossweiner, L. I. (1975) The oxidation of tryptophan by radical anions, *Int. J. Radiat. Biol. 27*, 201−204.
11. Adams, G. E. (1973) Radiation chemical mechanisms in radiation biology, in *Advances in Radiation Chemistry* (Burton, M., and Magee, J. L., Eds.), pp 125−207, John Wiley and Sons, New York, NY.
12. Havel, R. J., Eder, H. A., and Bragdon, J. H. (1955) The distribution and chemical composition of ultracentrifugally separated lipoproteins in human serum, *J. Clin. Invest. 34*, 1345−1353.
13. Filipe, P., Haigle, J., Freitas, J. P., Fernandes, A., Mazière, J.-C., Mazière, C., Santus, R., and Morlière, P. (2002) Anti- and pro-oxidant effects of urate in copper-induced low-density lipoprotein oxidation, *Eur. J. Biochem. 269*, 5474−5483.
14. Atmeh, R. F., Shepherd, J., and Packard, C. J. (1983) Subpopulations of apolipoprotein A-I in human high-density lipoproteins their metabolic properties and response to drug therapy, *Biochim. Biophys. Acta 751*, 175−188.
15. Sowell, A. L., Huff, D. L., Yeager, P. R., Caudill, S. P., and Gunter, E. W. (1994) Retinol, alpha-tocopherol, lutein/zeaxanthin, beta-cryptoxanthin, lycopene, alpha-carotene, trans-beta-carotene, and four retinyl esters in serum determined simultaneously by reversed-phase HPLC with multiwavelength detection, *Clin. Chem. 40*, 411−416.
16. Aksnes, L. (1994) Simultaneous determination of retinol, alpha-tocopherol, and 25-hydroxyvitamin D in human serum by high performance liquid chromatography, *J. Pediatr. Gastroenterol. Nutr. 18*, 339−343.
17. Thurnham, D. I., Smith, E., and Flora, P. S. (1988) Concurrent liquid-chromatography assay of retinol, α-tocopherol, *β*-carotene, α-carotene, lycopene and *β*-cryptoxanthin in plasma, with tocopherol acetate as internal standard, *Clin. Chem. 34*, 377−381.
18. Patterson, L. K., and Lilie, J. A. (1974) Computer-controlled pulse radiolysis system, *Int. J. Radiat. Phys. Chem. 6*, 129−141.
19. Hug, G. L., Wang, Y., Schoneich, C., Jiang, P. Y., and Fessenden, R. W. (1999) Multiple time scale in pulse radiolysis: applications to bromide solutions and dipeptides, *Radiat. Phys. Chem. 54*, 559−566.
20. Salmon, S., Mazière, J.-C., Santus, R., Morlière, P., and Bouchemal, N. (1990) UVB-induced photoperoxidation of lipids of human low and high density lipoproteins. A possible role of tryptophan residues, *Photochem. Photobiol. 52*, 541−545.
21. Schuler, R. H., Patterson, L. K., and Janata, E. (1980) Yield for the scavenging of OH radicals in the radiolysis of N_2O-saturated aqueous solutions, *J. Phys. Chem. 84*, 2088−2089.
22. Reyftmann, J.-P., Santus, R., Mazière, J.-C., Morlière, P., Salmon, S., Candide, C., Mazière, C., and Haigle, J. (1990) Sensitivity of tryptophan and related compound to oxidation induced by lipid autoperoxidation. Application to human serum low and high density lipoproteins, *Biochim. Biophys. Acta 1042*, 159−167.
23. Filipe, P., Morlière, P., Patterson, L. K., Hug, G. L., Mazière, J.-C., Mazière, C., Freitas, J. P., Fernandes, A., and Santus, R. (2002) Repair of amino acid radicals of apolipoprotein B100 of low-density lipoproteins by flavonoids. A pulse radiolysis study with quercetin and rutin, *Biochemistry 41*, 11057−11064.
24. Law, S. W., and Brewer, H. B., Jr. (1984) Nucleotide sequence and the encoded amino acids of human apolipoprotein A-I mRNA, *Proc. Natl. Acad. Sci. U.S.A. 81*, 66−70.
25. Knott, T. J., Priestley, L. M., Urdea, M., and Scott, J. (1984) Isolation and characterisation of a cDNA encoding the precursor for human apolipoprotein AII, *Biochem. Biophys. Res. Commun. 120*, 734−740.
26. Weinstein, M., Alfassi, Z. B., Defelippis, M. R., Klapper, M. H., and Farragi, M. (1991) Long range electron transfer between tyrosine and tryptophan in hen egg-white lysozyme, *Biochim. Biophys. Acta 1076*, 173−178.
27. Butler, J., Land, E. J., Prutz, W. A., and Swallow, A. J. (1982) Charge transfer between tryptophan and tyrosine in proteins, *Biochim. Biophys. Acta 705*, 150−162.
28. Jore, D., Patterson, L. K., and Ferradini, C. (1986) Pulse radiolytic study of α-tocopherol radical mechanisms in ethanolic solution, *J. Free Radical Biol. Med. 2*, 405−410.
29. Bisby, R. H., and Parker, A. W. (1991) Reactions of the α-tocopheroxyl radical in micellar solutions studied by nanosecond laser flash photolysis, *FEBS Lett. 290*, 205−208.
30. Davies, M. J., Forni, L. G., and Wilson, R. L. (1988) Vitamin E analogue Trolox C. E.S.R. and pulse-radiolysis studies of free-radical reactions, *Biochem. J. 255*, 513−522.
31. Noguchi, N., and Niki, E. (1998) Dynamics of vitamin E action against LDL oxidation, *Free Radical Res. 28*, 561−572.
32. Edge, R., McGarvey, D. J., and Truscott, T. G. (1997) The carotenoids as anti-oxidants−a review, *J. Photochem. Photobiol. B: Biol. 41*, 189−200.
33. Böhm, F., Edge, R., Land, E. J., McGarvey, D. J., and Truscott, T. G. (1997) Carotenoids enhance vitamin E antioxidant efficiency, *J. Am. Chem. Soc. 119*, 621−622.
34. Santus, R., Patterson, L. K., Hug, G. L., Bazin, M., Mazière, J.-C., and Morlière, P. (2000) Interactions of superoxide anion with enzyme radicals: kinetics of reaction with lysosyme tryptophan radicals and corresponding effects on tyrosine electron transfer, *Free Radical Res. 33*, 383−391.
35. Santus, R., Patterson, L. K., and Bazin, M. (1995) The diffusion-controlled reaction of semioxidized tryptophan with the superoxide radical-anion, *Free Radical Biol. Med. 19*, 837−842.
36. Cadenas, E., Merényi, G., and Lind, J. (1989) Pulse radiolysis study on the reactivity of Trolox C phenoxyl radical with superoxide anion, *FEBS Lett. 253*, 235−238.
37. Cudina, I., and Josimovic, L. (1987) The effect of oxygen on the radiolysis of tyrosine in aqueous solutions, *Radiat. Res. 109*, 206−215.
38. Macdonald, D. L., Terry, T. L., Agellon, L. B., Nation, P. N., and Francis, G. A. (2003) Administration of tyrosyl radical-oxidized HDL inhibits the development of atherosclerosis in apolipoprotein E-deficient mice, *Arterioscler., Thromb., Vasc. Biol. 23*, 1583−1588.
39. Sattler, W., Mohr, D., and Stocker, R. (1994) Rapid isolation of lipoproteins and assessment of their peroxidation by high-performance liquid chromatography postcolumn chemiluminescence, *Methods Enzymol. 233*, 469−489.
40. Francis, G. A. (2000) High density lipoprotein oxidation: *in vitro* susceptibility and potential in vivo consequences, *Biochim. Biophys. Acta 1483*, 217−235.
41. Giessauf, A., Steiner, E., and Esterbauer, H. (1995) Early destruction of tryptophan residues of apolipoprotein B is a vitamin E-independent process during copper-mediated oxidation of LDL, *Biochim. Biophys. Acta 1256*, 221−232.
42. Hazell, L. J., Davies, M. J., and Stoker, R. (1999) Secondary radicals derived from chloramines of apolipoprotein B-100 contribute to HOCl-induced lipid peroxidation of low-density lipoproteins, *Biochem. J. 339*, 489−495.

43. Cogny, A., Atger, V., Paul, J. L., Soni, T., and Moatti, N. (1996) High-density lipoprotein 3 physicochemical modifications induced by interaction with human polymorphonuclear leucocytes affect their ability to remove cholesterol from cells, *Biochem. J. 314*, 285−292.
44. Neta, P., Huie, R. E., and Ross, A. B. (1988) Rate constants for reactions of inorganic radicals in aqueous solutions, *J. Phys. Chem. Ref. Data 17*, 1027−1284.
45. Wald, J. H., Krul, E. S., and Jonas, A. (1990) Structure of apolipoprotein A-I in in three homogeneous reconstituted hgh density lipoprotein particles, *J. Biol. Chem. 265*, 20037−20043.
46. Furtmüller, P. G., Burner, U., and Obinger, J. (1998) Reaction of myeloperoxidase compound I with chloride, bromide, iodide, and thiocyanate, *Biochemistry 37*, 17923−17930.
47. Wilson, R. L., Dunster, C. A., Forni, L. G., Gee, C. A., and Kittridge, K. J. (1985) Organic free radicals and proteins in biochemical injury: electron or hydrogen transfer reactions?, *Philos. Trans. R. Soc. London B 311*, 545−563.
48. Wardman, P. (1989) Reduction potentials of one-electron couples involving free radicals in aqueous solution, *J. Phys. Chem. Ref. Data 18*, 1637−1755.
49. Hevonoja, T., Pentikäinen, M. O., Hyvönen, M. T., Kovanen, P. T., and Ala-Korpela, M. (2000) Structure of low density lipoprotein (LDL) particles: basis for understanding molecular changes in modified LDL, *Biochim. Biophys. Acta 1488*, 189−210.
50. Ibdah, J. A., Lund-Katz, S., and Philips, M. C. (1989) Molecular packing of high-density and low-density lipoprotein surface lipids and apolipoprotein A-I binding, *Biochemistry 28*, 1126−1133.
51. Foucher, C., Lagrost, L., Maupoil, V., Le Meste, M., Rochette, L., and Gambert, P. (1996) Alterations of lipoprotein fluidity by non-esterified fatty acids known to affect cholesteryl ester transfer protein activity. An electron spin resonance study, *Eur. J. Biochem. 236*, 436−442.

BI602530G